

matographic analysis was at most 2-3% and was therefore not taken into account in the analysis of the data. Attempts to carry out the chromatographic analysis at 15 °C were unsuccessful because of extensive broadening of peaks.

Racemization rate constants ( $k$ ) at 20.2, 25.0, and 35.0 °C are 1.25, 2.48, and  $9.67 \times 10^{-5} \text{ s}^{-1}$ , with correlation coefficients of 0.999. Calculated activation parameters are given in the text.

**X-ray Crystallography.** Crystals of decakis(dichloromethyl)biphenyl containing 1 mol equiv of THF were obtained from tetrahydrofuran by slow evaporation at room temperature. The crystals of the solvate did not effloresce appreciably on standing in air at room temperature for several months. A crystal of approximately  $0.05 \times 0.20 \times 0.23 \text{ mm}^3$  was chosen for the X-ray measurements. Crystal data:  $\text{C}_{22}\text{H}_{10}\text{Cl}_{20}\text{C}_4\text{H}_4\text{O}$ ,  $M_r$  1051.0; monoclinic (space group  $P2_1/n$  assumed throughout);  $a = 17.296(5) \text{ \AA}$ ,  $b = 10.091(3) \text{ \AA}$ ,  $c = 21.731(5) \text{ \AA}$ ,  $\beta = 96.79(2)^\circ$ ,  $V = 3766(2) \text{ \AA}^3$ ,  $d_{\text{calcd}} = 1.85 \text{ g}\cdot\text{cm}^{-3}$ ,  $Z = 4$ . X-ray intensities were measured at  $193 \pm 3 \text{ K}$  on a Nicolet R3m four-circle diffractometer equipped with a nitrogen-flow cooling device by applying Cu  $K\alpha$  radiation ( $\lambda = 1.54178 \text{ \AA}$ ). A total of 5902 reflections were recorded with  $h, k \geq 0$  and with  $3^\circ \leq 2\theta \leq 110^\circ$ . Of these, 3570 with  $[|F_0| > 3\sigma(F_0)]$  were considered unique and observed. Absorption corrections were ap-

plied analytically by approximating the crystal shape as a rectangular plate. The structure was solved by direct methods with the SHELXTL software. All non-hydrogen atoms were refined anisotropically, and hydrogen atoms were included at ideal positions ( $\text{C}-\text{H} = 0.96 \text{ \AA}$  and  $\text{C}-\text{C}-\text{H} = 109.5, 120.0^\circ$ ). The oxygen scattering factor was assigned to each position in the THF ring and refined; in all positions other than that near H(17) the  $R$  factor was ca. 0.4% higher.  $R$  and  $R_w$  after refinement were 0.057 and 0.047, respectively.

**Acknowledgment.** We thank the National Science Foundation (Grant CHE-8510067) for support of this work.

**Registry No.** 1, 112375-38-9; (+)-1, 112375-40-3; (-)-1, 112375-39-0; decamethylbiphenyl, 18356-20-2.

**Supplementary Material Available:** Bond lengths and bond angles, with standard deviations for 1 (Tables III and IV), final anisotropic thermal parameters for non-hydrogen atoms (Table V), and atomic and thermal parameters for hydrogen (Table VI) (4 pages). [The structure factor table is available from the author.] Ordering information is given on any current masthead page.

## Photoaddition and Photoreduction of Chloranil with Arenes via Singlet and Triplet Excited Complexes: Effects of Irradiation Wavelength and Radical Ion Pair Spin Multiplicity

Guilford Jones, II,\* William A. Haney, and Xuan T. Phan

Contribution from the Department of Chemistry, Boston University, Boston, Massachusetts 02215. Received July 24, 1986

**Abstract:** The photochemistry of chloranil (Q) in the presence of the arenes hexamethylbenzene, 1-methyl-, 1,3-dimethyl-, 1,4-dimethyl-, and 2,3-dimethylnaphthalene, and acenaphthene has been investigated. Irradiation in a nonpolar solvent provided ether adducts resulting from formal addition of the quinone to the arene side chain, the hydroquinone, (QH<sub>2</sub>), and in one case, an identifiable oxidation product, acenaphthylene. The quantum yield for these transformations was shown to have a complex dependence on the concentration of the arene and the irradiation wavelength. On irradiation at 366 nm under conditions in which free chloranil absorbs, the preferred product was the reduced species, QH<sub>2</sub>. On irradiation at 436 nm under conditions in which the ground-state charge-transfer (CT) complex of Q and the arene chiefly absorbs, the preferred product was the ether adduct. Excitation of complexes at 546 nm resulted in a sharply reduced quantum yield. Flash photolysis studies show that the quenching of Q triplets by the arenes leads to free radicals (QH<sup>•</sup> and DH<sup>•</sup>) by a sequential electron-transfer, proton-transfer mechanism. Irradiation of Q/DH<sub>2</sub> complexes appears alternatively to lead to singlet radical ion pairs (Q<sup>•-</sup>, DH<sub>2</sub><sup>•+</sup>) which evolve into singlet radical pairs (QH<sup>•</sup>, DH<sup>•</sup>) and final products in competition with back reactions which return radical pairs to ground-state reactants. The wavelength dependence of product quantum yield for excitation of Q/DH<sub>2</sub> complexes is discussed in terms of the facilitation of proton transfer within radical ion pairs due to the ability of side-chain C-H bonds of the arenes to act as acceptor modes for deposition of excess vibrational energy in charge transfer excited states.

The photochemistry of the "high-potential" quinone, chloranil (Q), was shown in early studies to involve photoaddition reactions and hydrogen atom abstraction from a variety of substrates (e.g., alcohols and aldehydes).<sup>1</sup> In more recent investigations molecular rearrangements that proceed via radical cation intermediates have been observed as the result of reductive quenching of the Q triplet excited state.<sup>2</sup> Several studies that have employed picosecond or nanosecond time-resolved laser flash techniques have led to the identification of transient species on electron transfer between <sup>3</sup>Q and aromatic hydrocarbons.<sup>3</sup> Although the tendency for quinones

to form ground-state complexes with potential reactants is well-known,<sup>4</sup> the importance of excitation of complexes in chloranil photochemistry is not well understood. In the early investigations of chloranil photochemistry,<sup>1</sup> there are intimations of the importance of ground-state quinone complexes in photoaddition reactions (unusual concentration dependences). In a recent phototransient and CIDNP study of indene complexes of Q, only the route involving excitation of uncomplexed Q and triplet quenching was verified for photolysis of Q in the presence of moderate concentrations of the electron donors.<sup>3a</sup>

In a series of investigations of the photochemistry of ground-state, charge-transfer (CT) complexes of varied electron donors and acceptors, a wavelength dependence of product quantum yields has been observed.<sup>2c</sup> This unusual dynamical feature for excited complexes (CT\*) shows considerable generality (e.g., electron transfer induced hydrocarbon rearrangements<sup>5</sup> and ionic disso-

(1) For a general review, see: Bruce, J. M. In *The Chemistry of Quinonoid Compounds*; Patai, S., Ed.; Wiley: New York, 1974; Part 1, Chapter 9.

(2) (a) Roth, H. D.; Schilling, M. L. M. *J. Am. Chem. Soc.* **1984**, *106*, 6053. (b) Roth, H. D.; Schilling, M. L. M. *Ibid.* **1981**, *103*, 1246. (c) Jones, G., II; Becker, W. G. *Chem. Phys. Lett.* **1982**, *85*, 271. (d) Jones, G., II; Chiang, S.-H.; Becker, W. G.; Welch, J. A. *J. Phys. Chem.* **1982**, *86*, 2805.

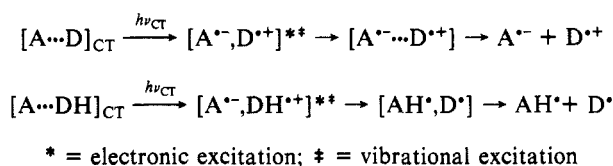
(3) (a) Rentzepis, P. M.; Steyert, D. W.; Roth, H. D.; Abelt, C. J. *J. Phys. Chem.* **1985**, *89*, 3955. (b) Kobashi, H.; Funabashi, M.; Kondo, T.; Morita, T.; Okada, T.; Mataga, N. *Bull. Chem. Soc. Jpn.* **1984**, *57*, 3557. (c) Gschwind, R.; Haselbach, E. *Helv. Chim. Acta* **1979**, *62*, 941.

(4) See: Foster, R. In ref 1, Chapter 7.

(5) (a) Jones, G., II; Becker, W. G. *J. Am. Chem. Soc.* **1983**, *105*, 1269. (b) *Ibid.* **1983**, *105*, 1276.

ciation of complexes or ion pairs of methylviologen<sup>6</sup>). The origin of the wavelength dependence can be identified with the evolution of contact ion pairs into solvent-separated ion pairs, which is facilitated by the deposition of excess vibrational energy in the intermolecular "stretch" that separates a contact ion pair (or the participation of solvent modes as acceptor vibrations) (Scheme I).<sup>5,6</sup>

## Scheme I



In further studies of this phenomenon we wished to identify other reaction paths that could show a similar dependence on excitation wavelength. Key features appear to involve the broad absorption bands available for excitation of organic CT complexes which provide access to Frank-Condon states with energies and nuclear geometries far removed from the relaxed excited species, CT\*. Nonetheless, one is confronted with the dominant mode of decay for excited CT complexes, reverse electron transfer, which returns aggregates to the ground state in subnanosecond time.<sup>3a,b,7</sup> A candidate for fast reaction from vibrationally "hot" excited CT states in competition with reverse electron transfer is transfer of a proton (Scheme I). This alternative could be most readily examined for systems employing a nonpolar solvent where ionic dissociation is not a competitor. A wavelength dependence then would be revealed in the enhanced formation of free radical species (and radical-derived products) on irradiation of CT complexes at high frequencies within the charge-transfer band. A number of quinone complexes appeared to be ideally suited for an electron-transfer, proton-transfer sequence.

There is currently much interest in the dynamics of formation and separation of charge for quinone moieties that are linked with porphyrin and other groups.<sup>8</sup> These model photochemical systems provide insight into the features of electron transport in natural photosynthesis. Of additional interest to our study is the current attention given to the general importance of sequential electron-proton transfer, which appears to play a mechanistic role for a variety of organic photochemical transformations.<sup>9</sup>

In the current paper we describe the behavior of chloranil and a series of electron-donor arenes. The arenes, alkylated derivatives of benzene and naphthalene, were selected to demonstrate sequential electron-proton transfer and to provide some comparison of donors that could readily provide sites for one- and two-electron oxidation in combination with the quinone. This system provides an interesting comparison of associates of the quinone with a "near neighbor" generated either through quenching of the quinone triplet or through aggregation in the ground state. We show that the evolution of radical pairs and the mechanism of electron transfer is in fact dependent on these modes of bimolecular quinone interaction and on the excitation wavelength as proposed. The present product and quantum yield study also provides a comparison for the flash photolysis investigations of Q and various electron donors recently reported<sup>10,11</sup> in which quinone triplet excited complexes have been identified. The work is related as well to recent reports of the photoreduction of chloranil in the

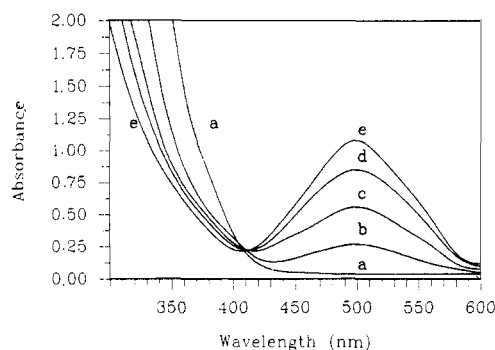


Figure 1. Absorption spectra obtained on addition of hexamethylbenzene (HMB) to chloranil (1.0 mM) in benzene with the following values of [HMB]: (a) 0 M; (b) 0.08 M; (c) 0.20 M; (d) 0.40 M; (e) 0.55 M.

## Chart I

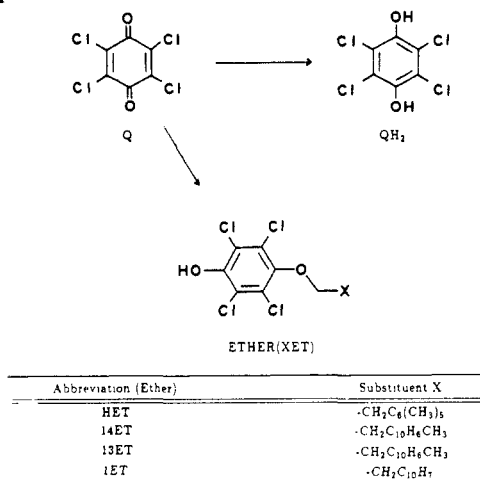


Table I. Absorption and Complexation Data for Q/DH<sub>2</sub> Complexes<sup>d</sup>

DH <sub>2</sub>	[Q], M	λ <sub>max</sub> <sup>CT</sup> , nm	K <sub>CT</sub> <sup>CT</sup> , M <sup>-1</sup>	ε <sub>CT</sub> <sup>CT</sup> , M <sup>-1</sup> cm <sup>-1</sup>	s <sup>b</sup>	[DH <sub>2</sub> ]/[Q] <sup>c</sup>
HMB	0.0010	460 <sup>d</sup>	3.2	1400	0.18–0.56	67–400
HMB	0.0010	510	2.8	2200	0.16–0.53	67–400
HMB	0.0010	560 <sup>d</sup>	2.8	1600	0.16–0.53	67–400
1MN	0.0013	500	0.62	1100	0.13–0.47	180–1100
14DMN	0.0010	530	0.83	900	0.18–0.37	40–260
23DMN	0.0024	520	0.62	600	0.06–0.33	42–330
NP	0.0024	480	0.39	600	0.04–0.22	42–290
ACN	0.0010	550	0.89	590	0.21–0.47	290–1000

<sup>a</sup> Solvent: benzene. <sup>b</sup> s ≈ K<sub>CT</sub>[DH<sub>2</sub>]/(1 + K<sub>CT</sub>[DH<sub>2</sub>]), where DH<sub>2</sub> is component in excess. <sup>c</sup> [DH<sub>2</sub>]/[Q] is the ratio of the excess component to the dilute component for the range of donor concentrations employed. <sup>d</sup> Absorbance data recorded at red and blue edges of CT band (Figure 1).

presence of cyclopolyenes,<sup>12</sup> for which the electron-proton-transfer sequence also appears to be important.

## Results

**Spectral Properties of the Chloranil/Arene System and Photoproduct Studies.** Addition of moderate concentrations (>50 mM) of the hydrocarbons hexamethylbenzene (HMB), 1-methylnaphthalene (MN), 1,3-dimethylnaphthalene (13DMN), 1,4-dimethylnaphthalene (14DMN), 2,3-dimethylnaphthalene (23DMN), and acenaphthene (ACN) to a 1 mM solution of chloranil (Q) in benzene or a 1,2,4-trichlorobenzene (TCB) resulted in the appearance of a visible absorption band ascribed to a CT transition for Q/arene complexes. Similar complexes involving Q and molecules with relatively low ionization potentials have been widely reported.<sup>13</sup> A typical CT absorption is shown

(6) Jones, G., II; Malba, V. *Chem. Phys. Lett.* **1985**, *119*, 105.

(7) (a) Peters, K. S.; Goodman, J. L. *J. Am. Chem. Soc.* **1985**, *107*, 1441.

(b) Hiliński, E. F.; Masnovi, J. M.; Kochi, J. K.; Rentzepis, P. M. *Ibid.* **1984**, *106*, 8071.

(8) See, for example: Gust, D., et al. *J. Am. Chem. Soc.* **1987**, *109*, 846 and references cited therein.

(9) Fox, M. A. *Adv. in Photochem.* **1986**, *13*, 237. (b) Lewis, F. D. *Acc. Chem. Res.* **1986**, *19*, 401.

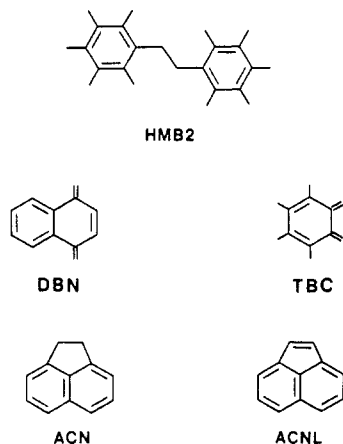
(10) (a) Levin, P. P.; Kokrashvili, T. A.; Kuz'min, V. A. *Izv. Akad. Nauk SSSR* **1983**, 284. (b) Peturshenko, K. B.; Vokin, A. I.; Turchaninov, V. K.; Gorshkov, A. G.; Frolov, Y. L. *Ibid.* **1985**, 267.

(11) Jones, G., II; Mouli, N.; Haney, W. A., in preparation.

(12) Jones, G., II; Haney, W. A. *J. Phys. Chem.* **1986**, *90*, 5410.

**Table II.** Product Yields from Hanovia Photolysis of Q/DH<sub>2</sub> in Benzene

DH <sub>2</sub>	[DH <sub>2</sub> ], M	time, h	product	yield, %
HMB	0.055	17	HET	81
			QH <sub>2</sub>	12
14DMN	0.036	4	14ET	53
			QH <sub>2</sub>	17
1MN	0.078	22	1ET	49
			QH <sub>2</sub>	trace
13DMN	0.036	5	13ET	70
23DMN	0.071	16	QH <sub>2</sub>	61
ACN	0.043	18	ACNL	19
			QH <sub>2</sub>	68

**Chart II**

in Figure 1, and other data concerning the complexes are provided in Table I, including the determination of association constants ( $K_{CT}$ ) and extinction coefficients ( $\epsilon_{CT}$ ) for the arene complexes (see Experimental Section for details).

For the purposes of exploratory studies and product identification, photolysis of Q/arene solutions in benzene was carried out by using the output of a Hg lamp, uranium glass filter (>330 nm), and conventional immersion well apparatus. The results of preparative photolysis are shown in part in Table II. The progress of photolysis to high conversion with a broad-band spectral source is in fact only a preliminary indicator of primary photochemical events. Under these conditions, light is absorbed not only by the complexes but by "free" chloranil.<sup>13</sup> In addition, as photolysis proceeded, the progress of reaction appeared to slow as indicated by the monitoring of products by HPLC and the bleaching of the principal absorption bands. A "quenching" of quinone reactions is known to commonly occur under circumstances in which the hydroquinone (QH<sub>2</sub>) is a significant product due to the quenching of quinone triplets by the hydroquinone.<sup>1</sup> In addition, TLC analysis revealed several products, which remained unidentified, and some polymer formation was suggested by the appearance of insoluble material on lengthy irradiation. Nonetheless, the major products of irradiation of Q/arenes were tetrachloro-hydroquinone (QH<sub>2</sub>) and a series of ethers (XET) that are formally adducts of the quinone and a side-chain C-H bond of the arene (Chart I).

The XET ether adducts were identified by NMR, IR, and mass spectral analysis (see Table III) and on the basis of comparison with products of thermal oxidation by chloranil of methylated aromatics.<sup>14</sup> The mass spectra showed a consistent base peak associated with fragmentation to an arylmethyl cation as shown

(13) (a) Foster, R. *Organic Charge-Transfer Complexes*; Academic: New York, 1969. (b) Benzene was selected as a solvent for its negligible photo-reactivity with chloranil. Although the weak complex of benzene and Q is known,<sup>4</sup> there is preferential complexation of Q with the arenes that are better donors. CT spectra and values of  $K_{CT}$  for Q/arenes in C<sub>6</sub>H<sub>6</sub> are similar to data for a noncomplexing solvent (e.g., TCB). Reference to "free chloranil" in C<sub>6</sub>H<sub>6</sub> is to be interpreted advisedly.

(14) Becker, H.-D. In *The Chemistry of the Quinonoid Compounds*; Patai, S., Ed.; Wiley: New York, 1974; Part 1, Chapter 7.

**Table III.** Ether Adducts from Hanovia Photolysis of Q/DH<sub>2</sub>

ether	mp, °C	<sup>1</sup> H NMR <sup>a,b</sup> δ	MS <sup>c</sup>	elem anal., %	
				theor	found
1ET	184	δ 8.5 m (1 H)	142 (0.26)	C (52.61)	C (52.52)
		7.7 m (6 H)	141 (1.00)	H (2.60)	H (2.48)
		5.6 s (2 H)	140 (0.32)	Cl (36.54)	Cl (36.28)
		3.8 s (1 H)	115 (0.55)		
14ET	189	δ 8.6 m (1 H)	156 (0.18)	C (53.77)	C (53.63)
		8.2 m (1 H)	155 (1.00)	H (3.01)	H (3.09)
		7.6 m (1 H)	154 (0.15)	Cl (35.27)	Cl (35.17)
		6.8 s (1 H)	128 (0.10)		
		5.4 s (2 H)	115 (0.09)		
		2.7 s (3 H)	115 (0.10)		
13ET	192	δ 8.3 m (1 H)	156 (0.16)	C (53.77)	C (54.02)
		7.6 m (5 H)	155 (1.00)	H (3.01)	H (3.20)
		5.4 s (2 H)	154 (0.15)		
		2.5 s (3 H)	128 (0.10)		
			115 (0.10)		
HET	192	δ 5.8 s (1 H)	162 (0.20)	C (52.97)	C (52.92)
		5.3 s (2 H)	161 (1.00)	H (4.45)	H (4.48)
		2.5 s (6 H)	160 (0.21)	Cl (34.74)	Cl (34.66)
		2.4 s (9 H)	91 (0.13)		
			41 (0.18)		

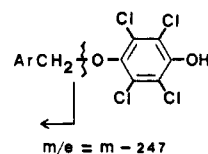
<sup>a</sup> CDCl<sub>3</sub> solvent (HET and 13ET), acetone-*d*<sub>6</sub> (14ET and 1ET).  
<sup>b</sup> Note deshielded hydrogens (1 H) at peri-naphthalene positions. <sup>c</sup> *m/e* (relative intensity).

**Table IV.** Product Quantum Yields<sup>a</sup> from Steady-State Photolysis of Q/DH<sub>2</sub> in Benzene

DH <sub>2</sub>	[DH <sub>2</sub> ], M	λ <sub>exc</sub>	φ(QH <sub>2</sub> )	φ(ether)	
HMB	0.002	366	0.097	0.022	
14DMN	0.005	366	0.041	0.018	
	0.003	366	0.044	0.017	
1MN	0.005	366	0.021	0.013	
HMB	0.200	436 <sup>b</sup>	0.019	0.078	
	14DMN	0.200	436 <sup>b</sup>	0.015	0.055
		0.400	436 <sup>b</sup>	0.018	0.062
1MN	0.550	436 <sup>b</sup>	0.008	0.046	

<sup>a</sup> Reproducibility ±15%. Irradiation into the Q/DH<sub>2</sub> bands at 546 nm was also carried out, but in all cases yields were negligible ( $\phi \leq 0.001$ ). [Q] = 0.005 M. <sup>b</sup> Percent *hν* absorbed by the CT complex vs free chloranil ( $\epsilon_{436} = 90 \text{ M}^{-1} \text{ cm}^{-1}$ ) was ≥90%.

below. A single isomer was identified for the adduct of Q and 13DMN; the NMR displayed a characteristically deshielded ( $\delta \sim 8.3$ ) C-8 naphthalene hydrogen similar to other adducts (note Experimental Section, Table III).



Oxidation products that would match the yields of photoreduction of the quinone were not isolated for the methylated aromatics. In principle, products of the quinodimethane type<sup>15</sup> would be possible such as 1,4-dihydro-1,4-dimethylenenaphthalene (DBN) or 3,4,5,6-tetramethyl-1,2-dimethylene-3,5-cyclohexadiene (TBC). DBN, for example, is a known structure which has been prepared in a low-temperature matrix ( $\lambda_{\text{max}} = 310 \text{ nm}$ ) but which is unstable due to polymerization above glass temperatures.<sup>16,17</sup> Another type of product is the "dehydro dimer" of the arene such as HMB2. This product was in fact prepared independently and shown not to appear as a photoproduct on careful HPLC analysis

(15) (a) See: Patai, S., Ed. *The Chemistry of the Quinonoid Compounds*; Wiley: New York, 1974; Part 2, Chapter 18. (b) Oppolzer, W. *Synthesis* 1978, 793.

(16) Pearson, J. M.; Six, H. A.; Williams, D. J.; Levy, M. *J. Am. Chem. Soc.* 1971, 93, 5034.

(17) A species such as DBN was not observed in the parallel flash photolysis study.<sup>11</sup> Its spectrum would appear in a difficult region of strong Q absorption.

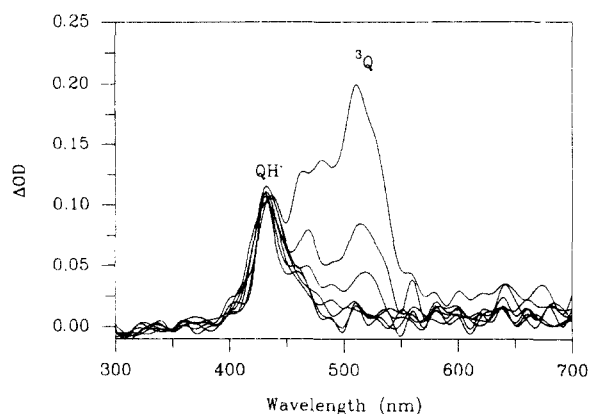


**Figure 2.** Transient spectra from 355-nm laser flash photolysis of 2.0 mM chloranil and 0.4 mM acenaphthene (ACN) in trichlorobenzene. Assignments for the quinone triplet state ( $^3Q$ ) and the semireduced quinone ( $QH^*$ ) are noted. Spectra correspond to decay times of 0.25 to 3.85  $\mu$ s following the laser pulse (600-ns intervals, descending absorbance at 510 nm).

of product mixtures at relatively low conversion (up to 10%). We conclude that structures as DBN and TBC are permissible products to accompany Q photoreduction and note that in the cases of 1MN and 13DMN, where dehydrogenation fails to provide a stable dehydrogenation or (closed shell) quinodimethane product, the formation of  $QH_2$  is suppressed.

**Quantum Yield Studies. Divergence of Product Yields and Ratios as a Function of Excitation Wavelength.** The appearance of the hydroquinone and ether products was monitored by HPLC for photolysis to low conversion using a monochromator-quantum counter system. Quantum yields for four of the arenes are shown in Table IV. For this analysis two sets of conditions were employed. One regime involved relatively low concentrations (2–5 mM) of arene so that the principal absorbing species ( $\geq 98\%$ ) at 366 nm was the uncomplexed quinone. Under these circumstances the Q triplet is generated with high efficiency from uncomplexed quinone,<sup>3</sup> and photoreduction proceeds by bimolecular encounter with arene.<sup>10,11</sup> For solutions with high [arene], it could be determined from the  $K_{CT}$  and  $\epsilon_{CT}$  data (Table I) that the principal absorbing species at 436 nm and 546 nm was the ground state complex of Q and arene. Notably, the quantum yield measurements for these two conditions provide a *fingerprint of reactivity* (Table IV), where differences well outside the experimental error (10–15%) are apparent. To further test the reversal in product quantum yields as a function of excitation wavelength, a subtle range of donor concentration was inspected for 14DMN. The data (Table IV) are consistent with the development of both reduction and addition products in both modes of photolysis. Therefore, the appearance of the minor product for 366- and 436-nm photolysis is not the result of competitive absorption, and the product fingerprint is cleanly that of Q triplet quenching and CT complex excitation, respectively.

Acenaphthene (ACN) was chosen as a donor in order to examine a system in which a product of two-electron oxidation by the quinone could be monitored. The solvent, 1,2,4-trichlorobenzene (TCB), provided a system that could be readily analyzed by GLC for the expected acenaphthylene (ACNL). In the event, the hydroquinone and ACNL were obtained in reasonable yield on preparative photolysis (Table II). Quantum yield determinations for the oxidation product, ACNL, were carried out with the following results: 366 nm ([ACN] = 2.0 mM,  $\phi = 0.11$ ); 436 nm ([ACN] = 0.30 M,  $\phi = 0.014$ ). These circumstances, in which, again, the photoredox product is disfavored for photolysis at high [arene], correspond to conditions in which the quinone is the principal absorber at 366 nm ( $>99\%$ ), whereas the CT complex played a primary role at 436 nm ( $>80\%$  absorption by the complex).

**Laser Flash Photolysis. Stepwise Electron-Proton Transfer for Quenching of Quinone Triplets.** Flash photolysis of several Q/arene systems was carried out by using the frequency-tripled output of

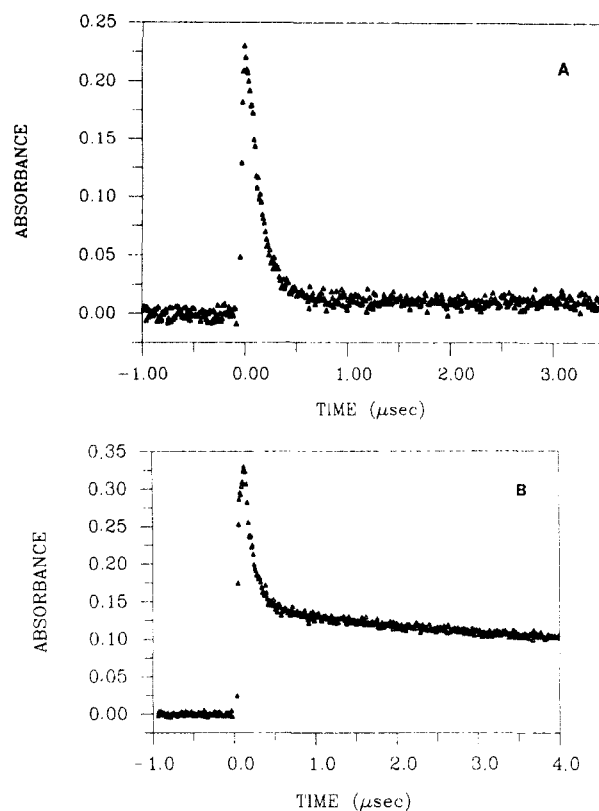
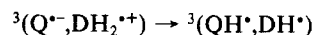


**Figure 3.** Transient absorption resulting from laser photolysis (355 nm) of 0.5 mM chloranil and 9.0 mM 1,4-dimethylnaphthalene (14DMN) in benzene: (A) transient decay at 660 nm (first order,  $\tau = 160$  ns); (B) transient decay at 435 nm.

a Nd:YAG laser (355 nm) as described previously.<sup>18</sup> For dilute deaerated solutions of Q and arene, the 510-nm transient<sup>3</sup> associated with the chloranil excited triplet is replaced within a few hundred nanoseconds with a more persistent absorption by the free radical, semireduced quinone ( $QH^*$ , 435 nm, ref 3), as shown in Figure 2 for Q/ACN. At intermediate concentrations of arene quencher (5–50 mM), at which absorption at 355 nm by ground-state Q/arene complexes is not important, other important intermediates can be observed. In Figure 3 are shown decay curves for transient inspection at two wavelengths, 435 and 660 nm, those associated with the  $QH^*$  and the radical anion,  $Q^{\cdot-}$  ( $\lambda_{max} = 450$  nm, ref 3) and the radical cation of substituted naphthalenes. This pair of absorptions is similar to that observed on quenching Q with naphthalene in acetonitrile, a polar solvent, which supports the formation of free radical ions.<sup>3c</sup>

Most notably for photolysis of Q/arenes at 355 nm in benzene, the 660-nm absorption decays relatively rapidly (unlike a free radical species), displaying first-order kinetics. For Q and 14DMN the calculated lifetime is 160 ns. On monitoring transient absorption at 435 nm, a bimodal decay is apparent, consistent with evolution of a Q/14DMN ion pair to a radical pair intermediate as follows:



The remaining absorption at 435 nm due to  $QH^*$  radicals is depleted in a longer time regime (100  $\mu$ s) with second-order kinetics. Photolysis at 355 nm of very concentrated solutions ([arene] = 0.2 M, conditions in which most of the Q is complexed) failed to give significant yields of either ion-pair or  $QH^*$  radical intermediates.

Of principal interest for the Q/ACN system (TCB solvent, Figure 2) was the direct measure of the quantum yield of free radicals, which could be compared with product quantum yields for steady photolysis. Following the procedure of Linschitz,<sup>19</sup>

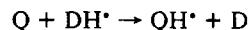
solutions of Q/ACN/TCB were compared with solutions of benzophenone in benzene having equal absorbance at 355 nm ( $OD = 0.80$ ). These solutions were alternately flashed at constant pulse energy (50 mJ), and the peak transient absorbance for benzophenone triplet (530 nm<sup>19</sup>) and the semiquinone radical (QH<sup>•</sup>, 435 nm) were recorded at a time at which neither transient was subject to significant decay. The average of several independent runs provided a value of 0.19 for the yield of QH<sup>•</sup>, based on the assumption of values for molar extinction coefficients for the transients (<sup>3</sup>BP,  $\epsilon = 7220 \text{ M}^{-1} \text{ cm}^{-1}$ ;<sup>19</sup> QH<sup>•</sup>,  $\epsilon = 7300 \text{ M}^{-1} \text{ cm}^{-1}$ <sup>3c</sup>). Decay of the QH<sup>•</sup> transient was shown to obey second-order kinetics. Several kinetic runs in which the quinone concentration was varied ( $[Q] = 0.5\text{--}5.0 \text{ mM}$ ) provided an average value of  $k/\epsilon = 1.9 \times 10^6 \text{ cm s}^{-1}$  and a rate constant for free radical (QH<sup>•</sup>) decay,  $k = 1.4 \times 10^{10} \text{ M}^{-1} \text{ s}^{-1}$ , assuming the reported value for  $\epsilon$ .

## Discussion

**Mechanism Involving the Quenching of Chloranil (Q) Triplets. Long-Lived Triplet Excited Complexes.** In several laser flash photolysis studies of Q, near-diffusion-limited quenching of the quinone triplet by aromatic hydrocarbons (including substituted naphthalenes and methylated benzenes) and other amine or heterocycle donors has been observed.<sup>3,10-12</sup> In a few instances, it has been possible to observe in the nanosecond time regime ion-pair intermediates which result from electron transfer, even in a nonpolar medium such as benzene or dichloroethane (e.g., Q quenching by durene,<sup>3b</sup> aromatic amines or heterocycles,<sup>10</sup> and methyl- and dimethylnaphthalenes<sup>11</sup>). An important feature of these systems, which will be discussed separately in more detail,<sup>11</sup> is the relatively long lifetime of the radical ion pair state, and its first-order decay which yields reactants and free QH<sup>•</sup> radicals (435 nm transient) (Figure 3). In another example, Q and 1-methylnaphthalene in benzene, an ion-pair transient having the Q<sup>•-</sup> and 1MN<sup>•+</sup> spectral signatures<sup>3d</sup> at 450 and 650–700 nm, respectively, and  $\tau = 140 \text{ ns}$  are observed.<sup>11</sup> The ion-pair intermediates generated in benzene almost certainly are highly electrostricted contact species, corresponding to the lowest triplet of the ground-state complex (triplet excited complexes, or TEC). One implication of the present divergent photolysis results is that the CT triplet is not an accessible excited state on direct irradiation into the CT band, but a novel species that can be sampled on bimolecular quenching of the free quinone triplet. Directly excited complexes are relegated to the singlet manifold, allowing only relatively fast in-cage processes to compete with rapid nonradiative decay to the ground state which occurs without intersystem crossing (100-ps time scale<sup>3a,b</sup>).

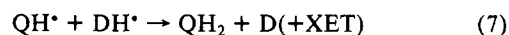
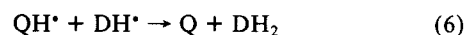
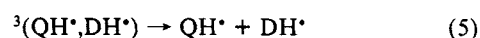
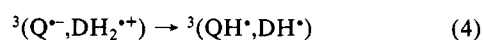
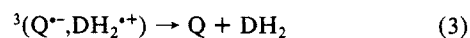
The mechanism proposed for formation of reduction (QH<sub>2</sub>) and addition products is shown in Scheme II. The proposal regarding TEC intermediates is appealing in providing a path for facile transfer for hydrogen as the proton within an ion pair, in competition with ion-pair intersystem crossing and decay to the ground state (steps 3 and 4). Recombination of neutral free radicals leads to the observed QH<sub>2</sub> and ether (XET) products. The product, D, a two electron oxidation derivative of the donor arene, DH<sub>2</sub>, is observed in the case of Q/ACN photolysis (ACN → ACNL). The yield of free radicals in this case ( $\phi = 0.19$ , flash measurement) is about double that of the quantum yield for QH<sub>2</sub> formation ( $\phi = 0.11$ , 366-nm steady irradiation) so that the recombination of radicals leading to reactants and products appears to be competitive.<sup>20</sup> The absence of a coupling product, HMB<sub>2</sub>, suggests that the selectivity in paths to photoredox and photoaddition products may be sensitive to steric factors. The preference for hydroquinone (QH<sub>2</sub>) product over the ethers revealed in low-conversion quantum yield determinations at 366 nm (Table IV) suggests that the cross reaction of QH<sup>•</sup> and DH<sup>•</sup> free radicals

generated via Q triplet quenching may operate at what is equivalent to a longer distance of radical-pair separation (a more remote or less oriented geometry of the components perhaps involving a coupled electron-proton transfer). Caged singlet radical pairs prepared on excitation of complexes (436-nm irradiation) then are understood to behave as more restricted species which show, by comparison, a propensity for radical coupling (favor for the ether product). Another mechanistic step of potential importance is the radical trapping



(and subsequent disproportionation of semiquinone radicals).<sup>1,21</sup> This alternative path is not in evidence in a more complicated decay of the QH<sup>•</sup> radical that might have been observed in flash photolysis experiments on Q/ACN.

## Scheme II



**Mechanism Involving Chloranil/Arene Charge-Transfer Complexes. Wavelength Effects.** The important features concerning the photoproduct and quantum yield studies include the following.

(1) The product ratio for irradiation at 436 nm (excitation of complexes) vs 366 nm (excitation of chloranil) is reversed, showing that product formation for the longer wavelength cannot result from a residual Q absorption and triplet quenching. The results are, moreover, consistent with quite distinct mechanisms of radical reaction, one emanating from triplet quenching and TEC intermediates and involving free radical recombination and the other employing singlet radical pairs reacting in-cage following CT excitation and intra-ion-pair proton transfer.

(2) HMB is a more efficient donor, particularly for the triplet mechanism (366-nm excitation quantum yields, Table IV), first because proton transfer is relatively more rapid vis-a-vis radical ion pair decay (e.g., step 4 vs step 3, Scheme II)<sup>21b</sup> and possibly because the secondary H-atom transfer (step 7) is more probable (statistical factor).

(3) Excitation well into the visible portion of the CT band (546 nm) is unproductive with regard to either type of product. In addition, flash photolysis (532 nm) of Q/arene complexes fails to produce any transients of significant lifetime ( $>100 \text{ ns}$ ).<sup>11</sup> Several levels of analysis show that the arene complexes are well-behaved stoichiometric entities, as has been commonly found for complexes of Q.<sup>4</sup> The Benesi-Hildebrand and related treatments of the absorbance/donor concentration data provided excellent linear plots (typically,  $r = 0.99$ ) and calculated association constants (Table I) were sizable (outside the range for "contact" complexes<sup>22</sup>). Consistent results were obtained from B-H plots for analysis at wavelengths also at the edges of the CT band for Q/HMB (note Table I and Figure 1). A Job's plot<sup>13a</sup> of the absorbance/mole fraction data was also consonant with a Q/HMB complex of 1:1 stoichiometry ( $OD_{\text{max}} = 0.5$ ). It is difficult then to argue that the wavelength effects could be associated with aggregates with different geometries or stoichiom-

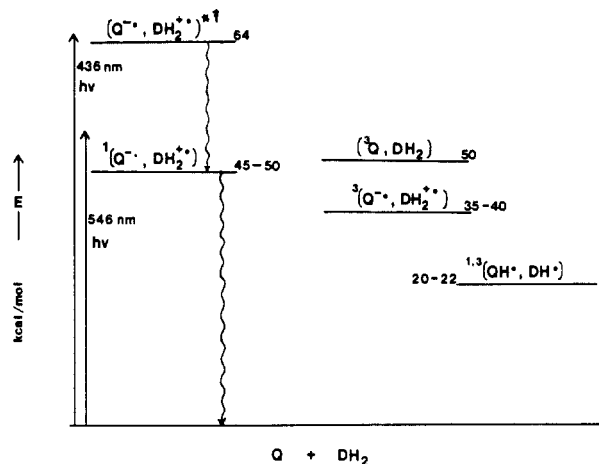
(19) Hurley, J. K.; Sinai, N.; Linschitz, H. *Photochem. Photobiol.* **1983**, *38*, 9.

(20) An ether adduct of ACN was not isolated in preparative irradiation and could give rise to ACNL by thermal reaction (GLC), accounting for some overall radical decay. From the transient OD's for QH<sup>•</sup> for other donors, radical yields appeared to be similarly high.<sup>11</sup>

(21) (a) In the related flash photolysis study,<sup>11</sup> quenching of the benzhydryl (ketyl) radical by ground-state Q could be observed. However, this path should involve coupling and (disfavored) ether (XET) product formation for the donor, 1MN, since the latter would not deliver a second hydrogen for photoreduction. (b) The TEC intermediate for Q/HMB shows a shorter lifetime (80 ns) and a higher QH<sup>•</sup> radical yield than either Q/14DMN or Q/1MN.

(22) Tamres, M.; Strong, R. L. In *Molecular Association*; Foster, R., Ed.; Academic: New York, 1979; Vol. 2, Chapter 5.

## Scheme III



eries or that the CT band is a composite of electronic transitions employing orbitals of donor and/or acceptor of different symmetry (selective excitation to species with different electronic configuration and reactivity). These factors would have to be fortuitously similar for the various arenes for which there is a consistent product pattern.

We will argue in favor of a wavelength dependence that is of a general nature involving CT complexes with well-defined equilibrium geometries and a common type of electronic transition. The wavelength dependence could depend in a simple way on energetics; i.e., relaxed excited complexes simply have insufficient energy to produce the radical products. In Scheme III the disposition of various species is presented. An estimate of the energy of the relaxed CT\* is made at the red edge of the CT absorption band (ca. 580–620 nm) (the complexes do not fluoresce at room temperature); a modest singlet–triplet splitting for CT\* is assumed. The chloranil triplet energy is approximately 50 kcal/mol.<sup>1</sup> The energy of the radical pair can be estimated by using values for an arene C–H bond dissociation energy of ca. 85 kcal/mol and a recently estimated value for the O–H bond energy in a QH• radical (the dissociation energy for removal of the second hydrogen from hydroquinone, 64 kcal/mol).<sup>23</sup> From this analysis (Scheme III) it appears that excitation at any point within the charge-transfer band is sufficiently energetic to drive the subsequent proton transfer. Another possibility is raised in terms of selective population of the local chloranil triplet from upper vibrational levels of CT\*. However, this mechanism would be likely to produce the <sup>3</sup>CT\* state <sup>3</sup>(Q•-, DH<sub>2</sub>•+), whose behavior (relatively long lifetime) has been independently assessed based on flash photolysis results for <sup>3</sup>Q quenching.<sup>10,11</sup>

We propose a direct path from vibrationally excited CT excited states (Scheme IV), a mechanism that takes into account the way in which excess excitation energy is distributed among normal vibrational modes of component molecules within a complex. The argument centers around the identification of high-frequency side-chain C–H stretching modes as acceptors of vibrational excitation which results through electronic excitation within Q/arene complexes. Shown in Figure 4, is a potential energy–nuclear configuration coordinate diagram which may be considered general for the various arenes. Notably, the equilibrium geometries for ground and excited complexes are displaced. This feature results from distention of C–H bonds as the result of charge-transfer excitation (formation of the donor radical cation) and attendant hyperconjugative stabilization of charge by ring substituent groups. In this model the important feature is the stretching of a C–H bond which results from excitation at higher frequencies within the CT band. The Frank–Condon state represents a species whose altered electronics render the side-chain hydrogens relatively acidic.<sup>24</sup> More energetic excitations also result in population of

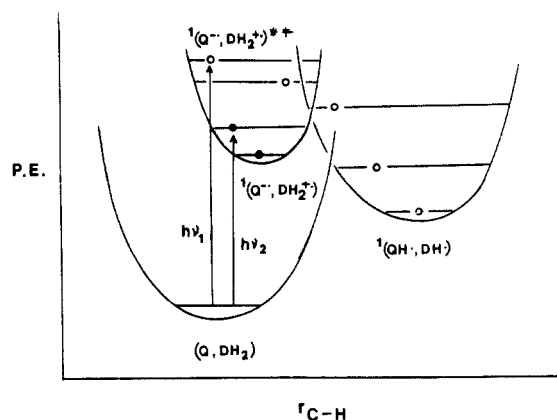
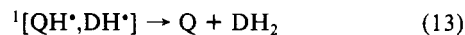
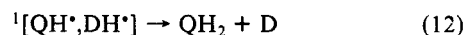
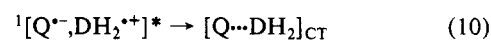
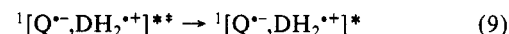
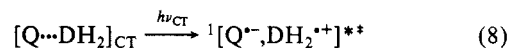


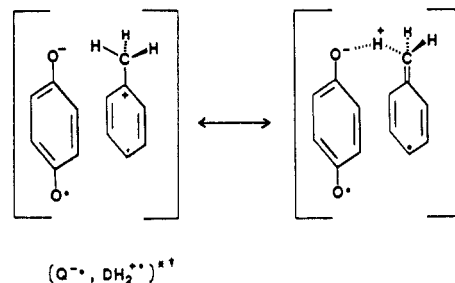
**Figure 4.** Potential energy–configuration coordinate diagram for the reaction of chloranil/arene excited CT complexes. The change in nuclear configuration represents an idealized view of stretching of a single C–H bond. The diagram depicts the motion of nuclei (representative points) after charge-transfer excitation to vibronic levels which are sufficiently energetic ( $h\nu_1$ , open circles) or insufficiently energetic ( $h\nu_2$ , filled circles) for proton transfer (radical ion pair  $\rightarrow$  radical pair transformation).

## Scheme IV



\* = electronic excitation; † = vibrational excitation

## Scheme V



vibrational levels in which one or more hydrogens are a component of a significantly stretched and weakened bond. A similar type of rationale has been made by Lim<sup>26</sup> concerning the activation of C–H acceptor mode in nonradiative decay, in a detailed study of fluorescence quantum efficiencies for arene CT complexes in the gas phase.

Shown in Figure 4 is an idealization of nuclear motion which depends on the excess energy present for different vibronic levels. Upper vibronic states have a higher probability of crossing the barrier for proton transfer (open circles) in competition with normal relaxation of the C–H stretch. Another way of viewing the vibronic population would take into account the avoided crossing of electronic potential energy curves, in which case higher frequency excitation results in population of vibronic levels which

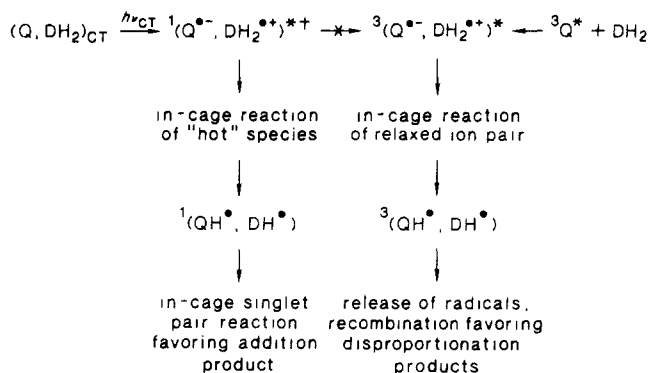
(23) Friedrich, L. E. *J. Org. Chem.* **1983**, *48*, 3851.

(24) The sharply enhanced acidity for benzylic hydrogens (e.g., for HMB<sup>•+</sup>,  $pK_a \sim 1$ , CH<sub>3</sub>CN) has been recently studied quantitatively.<sup>25</sup>

(25) (a) Schlesener, C. J.; Amatore, C.; Kochi, J. K. *J. Am. Chem. Soc.* **1984**, *106*, 7472. (b) Nicholas, A. M. P.; Arnold, D. R. *Can. J. Chem.* **1982**, *60*, 2165.

(26) (a) Lim, B. T.; Okajima, S.; Chandra, A. K.; Lim, E. C. *Chem. Phys. Lett.* **1981**, *79*, 22. (b) Okajima, S.; Lim, E. C. *J. Phys. Chem.* **1982**, *86*, 4120.

## Scheme VI



are dissociative with respect to proton migration (part of the continuum).

The important intermediate ( $Q^{\bullet-}, DH_2^{\bullet+}$ )<sup>\*\*</sup>, which is both electronically and vibrationally excited, is shown in Scheme V. This species is available only on CT excitation at shorter wavelengths. Included in the diagram are resonance structures for this Frank-Condon intermediate showing the lengthened C-H bond (a vibration which "follows" the electronic transition) and a resonance form taking into account the hyperconjugative interaction with the ring, which is important in stabilization of the radical cation moiety.<sup>27</sup> The geometry of this vibronic state in fact approximates the transition state for proton transfer if one assumes that a C-H stretching motion of this type occurs in the vicinity of the quinone moiety which will provide a proton acceptor site within the short lifetime of the vibronic state.<sup>28</sup>

The data for respective singlet and triplet excited complexes allow a unique comparison. It is assumed that the lifetime of the upper vibronic level populated on excitation at the blue edge of the Q/arene CT band is about 10 ps<sup>28</sup> and given that the quantum yield of proton transfer is on the order of 0.1 (from product quantum efficiency data), then the rate constant for proton transfer via the "hot" excited singlet complex is ca.  $10^{10} \text{ s}^{-1}$ . This value may indeed resemble the "barrier-free" rate constant (Arrhenius preexponential factor) for proton transfer and is to be compared with rate constants of  $(5-10) \times 10^6 \text{ s}^{-1}$  for the relaxed (thermalized) triplet (TEC) intermediate.<sup>3b,10,11</sup>

In summary, the photolysis of CT complexes of chloranil and the arenes results in photoreduction (QH<sub>2</sub>) and addition (XET) products. Notably, product quantum yields (ratios) differ with respect to the alternative mode of photolysis, i.e., excitation of uncomplexed quinone followed by <sup>3</sup>Q triplet quenching. Moreover, excitation at low frequencies within the CT band for the quinone complexes is ineffective in product formation, whereas excitation at the blue edge of the CT band results in moderately active photochemistry. These contrasting mechanisms are summarized in Scheme VI with regard to the entry to singlet and triplet radical ion pair species and their choices of routes to cage and escape products. The wavelength dependence for photolysis of Q complexes may be understood in terms of the population of vibronic states (through higher energy excitation), which results in the weakening of a side-chain C-H bond through hyperconjugative stabilization of the arene radical cation component of the excited complex. This selective "pumping" of vibrational levels has now been found for two types of processes that occur on a time scale that is fast enough to compete with normal radiationless deac-

(27) Some representative IP data that show stabilization of radical ions by the side chain are as follows: HMB, 7.94; C<sub>6</sub>H<sub>6</sub>, 9.24; 1MN, 7.96; NP, 8.12 eV. See: Miller, L. L.; Nordblom, G. D.; Mayeda, E. A. *J. Org. Chem.* **1972**, *37*, 916.

(28) (a) For discussion of lifetimes of upper vibronic levels and energy partitioning, see: Naaman, R.; Lubman, D. M.; Zare, R. N. *J. Mol. Struct.* **1980**, *59*, 225. Flynn, G. W. *Acc. Chem. Res.* **1981**, *14*, 334. Mataga, N. *Radiat. Phys. Chem.* **1983**, *21*, 83. (b) We consider possible a  $\lambda$  dependence mechanism that involves crossing of an upper singlet excited state (i.e., the involvement of an excited state of the product radical pair, [QH<sup>•</sup>, DH<sup>•</sup>]). For example, a low-lying state of the donor radical would provide an energetically feasible adiabatic proton transfer; yielding [QH<sup>•</sup>, DH<sup>•</sup>].

tivation of CT excited states involving reverse electron transfer. These processes include the present intra-ion-pair proton transfer, observable in nonpolar media, and the previously reported ionic dissociation of complexes observed for polar solvents.<sup>4-6</sup>

We are continuing to pursue the rather specialized photochemical mechanisms employed by CT complexes, particularly those involving the deposition of a large excess of vibrational energy which can be deployed in driving ultrafast reactions.

## Experimental Section

**Materials and Methods.** Baker HPLC-grade benzene (BZ) and acetonitrile (AN) were purified by fractional distillation under house vacuum (ca. 50 Torr) from P<sub>2</sub>O<sub>5</sub> and then stored over molecular sieves. Chloranil (Q) (Aldrich) was further purified by recrystallization from purified benzene three times, followed by vacuum sublimation at 1 Torr. Benzophenone (BP) was recrystallized from hexane, methanol, and finally petroleum ether. Tetrachlorohydroquinone (QH<sub>2</sub>) (Aldrich) was further purified by recrystallization from glacial acetic acid, washed with distilled water, dried under vacuum, and then vacuum sublimed. 1-Methylnaphthalene (1MN) (bp 240–241 °C) was fractionally distilled; 1,4-dimethylnaphthalene (14DMN) and 1,3-dimethylnaphthalene (13DMN) were used as supplied (Aldrich). The following solids were purified by recrystallization from absolute ethanol:naphthalene (NP) (mp 80–81 °C), hexamethylbenzene (HMB) (mp 164 °C), 2,3-dimethylnaphthalene (23DMN) (mp 103–104 °C), acenaphthene (ACN) (mp 96 °C), and acenaphthylene (ACNL) (mp 92–93 °C). ACN and ACNL were analyzed by GLC (Varian 3700 instrument) using a Scot-GSB column at 130 °C. In order to analyze for the "dehydro dimer" of HMB, an independent synthesis was carried out via a Grignard reaction.<sup>29</sup> Pentamethylbenzyl chloride (0.05 mol) was reacted with 0.05 mol of magnesium in anhydrous ether for 3 h followed by carbonation and acidification. Upon workup 2.5 g (35% yield) of 1,2-bis(pentamethylphenyl)ethane<sup>29</sup> (HMB2) was obtained (mp 240 °C).

**Laser Flash Photolysis.** The apparatus and procedures for Nd:YAG laser flash photolysis and transient detection have been previously described.<sup>18</sup> In addition to observation of Q triplet quenching by naphthalene derivatives,<sup>10c</sup> a determination of the yield of product-forming free radicals, QH<sup>•</sup>, was important to the present study. For determination of the quantum yield for formation of the semiquinone radical, photolysis of Ar-purged solutions of Q (1.0 mM) and acenaphthene (0.4 mM) in trichlorobenzene at 355 nm was carried out. Transient optical densities (435 nm), which reached a plateau value at ca. 5  $\mu\text{s}$  following the laser pulse, were compared with transient absorbances measured for similar irradiation of the benzophenone actinometer.<sup>19</sup> The BP triplet transient (535 nm) was monitored with respect to its maximum absorbance (50–200 ns following pulsed excitation); its quantum yield was assumed to be 1.0, and its molar absorptivity  $\epsilon = 7220 \text{ M}^{-1} \text{ cm}^{-1}$  (benzene).<sup>19</sup> Solutions of BP and Q/ACE were Ar purged and matched in terms of OD at 355 nm (0.80). Samples were subjected to 20 laser pulses, and transient data were collected and averaged via computer and a CAMAC interface (100-MHz digitization) as described.<sup>18</sup>

**Steady-State Photolysis: Hanovia System.** The apparatus consisted of a water-cooled quartz or Pyrex cold finger with a central well fitted with a 450-W medium-pressure mercury arc lamp and a uranium glass sleeve (for irradiations at  $\lambda > 330 \text{ nm}$ ). All irradiations were carried out under a nitrogen atmosphere with magnetic stirring. The results are summarized in Table II. Several sample procedures follow.

**Photolysis of Chloranil and Hexamethylbenzene.** A solution containing Q (1.0 g) and HMB (4.0 g) in benzene solvent (450 mL) was irradiated until the carbonyl IR absorption of Q ( $1696 \text{ cm}^{-1}$ ) diminished to a small intensity and the original red color of the solution was bleached to light yellow (ca. 17 h). The solvent was removed and the mixture chromatographed on a Florisil column with light petroleum ether, affording recovered HMB. Continued elution with benzene yielded a mixture (1.5 g) of two products, which were subsequently separated by preparative TLC (Silica, Chloroform solvent). The less polar product was the ether adduct of HMB and Q; 4-((pentamethylphenyl)methoxy)tetrachlorophenol (HET) (1.37 g, 81%) (mp 192 °C) (see Tables I and II), UV (CHCl<sub>3</sub>),  $\lambda_{\text{max}} = 300 \text{ nm}$  ( $\epsilon = 3650 \text{ M}^{-1} \text{ cm}^{-1}$ ). The more polar product was identified as QH<sub>2</sub> (0.12 g, 12%) by comparison with an authentic sample.

**Photolysis of Chloranil and 1-Methylnaphthalene.** Q (1.0 g) and 1MN (5.0 g) were dissolved in 450 mL of benzene and irradiated for 22.5 h. After rotary evaporation of solvent to a small volume and standing for several days, the photolysis mixture solidified. Recrystallization twice from aqueous alcohol and then once from cyclohexane afforded light tan plates of 4-(1-naphthylmethoxy)tetrachlorophenol (1ET) (0.67 g, 49%)

(29) Humphlett, W. J.; Hauser, C. R. *J. Am. Chem. Soc.* **1950**, *72*, 3289.



(mp 183–184 °C); UV ( $\text{CHCl}_3$ ),  $\lambda_{\text{max}} = 284 \text{ nm}$  ( $\epsilon = 9970 \text{ M}^{-1} \text{ cm}^{-1}$ ).  $\text{QH}_2$  was found only in trace amount.

**Photolysis of Chloranil and Acenaphthene.** A solution of Q (1.5 g) and ACN (3.0 g) in 450 mL of benzene was irradiated for 18 h. Solvent was removed and the residue taken up in acetonitrile for GLC analysis (Scot-GSB column, 130 °C), which showed ACN ( $R_t = 19.1 \text{ min}$ ) and ACNL ( $R_t = 15.8 \text{ min}$ ). The yield of ACNL was determined using an internal standard to be 19%. When benzene was added to the original photoproduct, a white solid precipitated, which was found to be  $\text{QH}_2$  (1.02 g, 68%). ACNL photodimer<sup>30</sup> was also detected but not analyzed quantitatively.

**Steady-State Photolysis: Monochromator System.** For determination of product quantum yields, the previously described apparatus<sup>5</sup> was used, the essential components of which are a light source, monochromator, and quantum counting device. The light source, an Oriol 500-W lamp, was focused onto the entrance slit (2.68 nm) of a Bausch and Lomb high-intensity monochromator (maximum band-pass = 9.6 nm). Typically a 2-mL solution of the sample was placed in a quartz cuvette with a magnetic stir bar, sealed with a septum, and then sparged with argon before irradiation in the monochromator apparatus with magnetic stirring. The products were analyzed by HPLC with reference to a calibration curve of integrated area versus concentration determined for the pure substance by an average of three runs under conditions identical with those described below for the irradiated samples.

The HPLC system used was a Rainin/Gilson HP/HPX with binary solvent delivery in conjunction with a Rainin Microsorb high-performance  $C_1$ , reversed-phase column and Apple IIe microprocessor. Sample injections were made via a Rheodyne 725 injector; a Kratos 757 variable-wavelength (190–800 nm) UV-vis detector was used. The HPLC solvent system was 100% Baker HPLC-grade methanol versus a mixture of 90% Millipore water (MilliQ system, with ion and carbon filters) and 10% methanol. The solvents were sparged with argon and then maintained under argon throughout the analytical runs. A HP 3380A plotting integrator was used for recording sample retention times as well as quantifying peaks through their integrated areas relative to an internal standard or with respect to a calibration curve of integrated area versus concentration. Irradiation times were generally from 8 to 64 min, with quantum yields determined from a plot of moles of product vs einsteins of light absorbed. The reported quantum yields are an average of duplicate independent measurements and were reproducible to within  $\pm 15\%$ . Sample runs are noted as follows.

**Photolysis of Chloranil and Hexamethylbenzene ( $\lambda_{\text{exc}} = 366 \text{ nm}$ ).** A 2-mL solution of Q (5 mM) and HMB (2 mM) in benzene was irradiated at 366 nm ( $A > 3$ ) in the monochromator apparatus for 8, 16, 32, and 64 min. The photolysis mixture was analyzed by HPLC with 43% methanol versus 90/10 HOH/MeOH at 4000 psi, a flow rate of 1.3 mL/min, and 0.01 absorbance unit full scale. For the 16-min irradiation, products, retention times, and integrated peak areas were as follows:  $\text{QH}_2$  ( $R_t = 14.10 \text{ min}$ , area =  $7.62 \times 10^4$  units), HET ( $R_t = 2.72 \text{ min}$ , area =  $8.52 \times 10^{-4}$  units). For product analysis a calibration curve of concentration vs integrated peak area was developed by injection of pure sample at successive dilution (three runs averaged, linear regression analysis [ $r = 0.999$ ]). For example,  $\text{QH}_2$  (1 mM =  $2.5 \times 10^5$  units),

HET (1 mM =  $1.05 \times 10^6$  units). The analysis gave quantum yield values as follows:  $\text{QH}_2$  ( $\phi = 0.097$ ), HET ( $\phi = 0.022$ ).

**Photolysis of Chloranil and Hexamethylbenzene ( $\lambda_{\text{exc}} = 436 \text{ nm}$ ).** A solution in benzene of 5 mM Q and 200 mM HMB was irradiated at 436 nm ( $A = 2.4$ ), where absorbance due to the CT band was  $\geq 90\%$ . HPLC analysis gave products, retention times, and integrated peak area as follows:  $\text{QH}_2$  ( $R_t = 14.00 \text{ min}$ , area =  $2.31 \times 10^4$  units), HET ( $R_t = 2.70 \text{ min}$ , area =  $4.69 \times 10^5$  units). Quantum yield analysis gave  $\text{QH}_2$  ( $\phi = 0.019$ ) and HET ( $\phi = 0.078$ ).

**Photolysis of Chloranil and 1,4-Dimethylnaphthalene ( $\lambda_{\text{exc}} = 366 \text{ nm}$ ).** A 2-mL solution of Q (5 mM) and 14DMN (5 mM) in benzene was irradiated at 366 nm ( $A > 3$ ) for 5, 16, 32, and 64 min. Product retention times, peak areas, and quantum yields for the 16-min irradiation were as follows:  $\text{QH}_2$  ( $R_t = 13.75 \text{ min}$ , area =  $3.41 \times 10^4$  units,  $\phi = 0.041$ ), 14ET ( $R_t = 3.47 \text{ min}$ , area =  $1.04 \times 10^5$ ,  $\phi = 0.018$ ).

**Photolysis of Chloranil and 1,4-Dimethylnaphthalene ( $\lambda_{\text{exc}} = 436 \text{ nm}$ ).** A solution in benzene of 5 mM Q and 300 mM 14DMN was irradiated at 436 nm ( $A = 2.24$ ), where absorbance due to the CT band was  $\geq 90\%$ . HPLC analysis gave products, retention times, and integrated peak areas as follows:  $\text{QH}_2$  ( $R_t = 14.00 \text{ min}$ , area =  $1.76 \times 10^4$  units), 14ET ( $R_t = 3.48 \text{ min}$ , area =  $4.39 \times 10^5$  units). Quantum yield analysis gave  $\text{QH}_2$  ( $\phi = 0.015$ ) and 14ET ( $\phi = 0.055$ ).

**Formation Constants for the Complexes: Chloranil/ $\text{DH}_2$ .** In order to obtain  $K_{\text{CT}}$  and  $\epsilon_{\text{CT}}$  values, the CT complex of Q (acceptor (A)) and each donor (D) was analyzed spectrophotometrically (see Figure 1) by several methods.<sup>13a</sup> Among these were the Benesi-Hildebrand, Foster, Scatchard, and Scot analyses. In each case change in optical density (OD) was recorded for a solution that was low in [A] while the donor was added stepwise to a large excess. Each of the values determined by the Benesi-Hildebrand analyses gave results for  $K_{\text{CT}}$  and  $\epsilon_{\text{CT}}$  that agreed within  $\pm 10\%$  with values obtained by the other plotting procedures. A saturation fraction ( $S$ ) was computed<sup>31</sup> ( $S = K_{\text{CT}}[D]/(1 + K_{\text{CT}}[D])$ ), since it has been shown that reliable values of  $K_{\text{CT}}$  and  $\epsilon_{\text{CT}}$  can be obtained when  $0.2 < S < 0.8$ . Values for  $K_{\text{CT}}$  and  $\epsilon_{\text{CT}}$  at  $\lambda_{\text{max}}^{\text{CT}}$  along with other statistical data having to do with the degree of "saturation" of the acceptor and the excess of donor are shown in Table I. A typical procedure is described in detail as follows. Six individual solutions of 0.0024 M Q in 2 mL of benzene were prepared with [HMB] = 0.08–0.48 M. The absorbance of each solution was measured at the  $\lambda_{\text{max}}$  of the CT absorption band (510 nm) from which a Benesi-Hildebrand plot of  $[Q]/A_{\text{CT}}$  vs  $1/[\text{HMB}]$  gave a linear plot with correlation coefficient = 0.999.

**Acknowledgment.** We thank the Office of Basic Energy Sciences of the Department of Energy for support of this work. Funds for laser facilities were also provided by the Department of Defense through its University Research Instrumentation Program. We also thank Dr. T. Kumagai, P. Weakliem, and N. Mouli for technical assistance.

**Registry No.** Q, 118-75-2; HMB, 87-85-4; MN, 90-12-0; 13DMN, 575-41-7; 14DMN, 571-58-4; 23DMN, 581-40-8; ACN, 83-32-9;  $\text{QH}_2$ , 87-87-6; HET, 112740-49-5; 14ET, 112740-50-8; 13ET, 112740-51-9; 1ET, 112740-52-0; ACNL, 208-96-8.

(30) Cowan, D. O.; Drisko, R. L. In *Elements of Organic Photochemistry*; Plenum: New York, 1976, p 435.

(31) Deranleau, D. *J. Am. Chem. Soc.* **1969**, *91*, 4044.